Journal of Fusion Energy, Vol. 12, No. 3, 1993

Reversed-Field Pinch Studies in the Madison Symmetric Torus

S. Hokin,[1] A. Almagri,[1] M. Cekic,[1] B. Chapman,[1] N. Crocker,[1] D. J. Den Hartog,[1] G. Fiksel,[1] J. Henry,[1] H. Ji,[1] S. Prager,[1] J. Sarff,[1] E. Scime,[1] W. Shen,[1] M. Stoneking,[1] and C. Watts[1]

Studies of large-size ($R = 1.5$ m, $a = 0.5$ m), moderate current ($I < 750$ kA) reversed-field pinch (RFP) plasmas are carried out in the Madison Symmetric Torus in order to evaluate and improve RFP confinement, study general toroidal plasma MHD issues, determine the mechanism of the RFP dynamo, and measure fluctuation-induced transport and anomalous ion heating. MST confinement scaling falls short of the RFP scaling trends observed in smaller RFPs, although the plasma resistance is classical. MHD tearing modes with poloidal mode number $m = 1$ and toroidal mode numbers $n = 5$–7 are prevalent and nonlinearly couple to produce sudden relaxations akin to tokamak sawteeth. Edge fluctuation-induced transport has been measured with a variety of insertable probes. Ions exhibit anomalous heating, with increases of ion temperature occurring during strong MHD relaxation. The anomalous heating fraction decreases with increasing density, such that ion temperatures approach the lower limit given by electron-ion friction. The RFP dynamo has been studied with attention to various possible mechanisms, including motion-EMF drive, the Hall effect, and superthermal electrons. The toroidal field capacity of MST will be upgraded during Summer 1993 to allow low-current tokamak operation as well as improved RFP operation.

KEY WORDS: Reversed-field pinch; MHD instability; anomalous transport; anomalous ion heating; dynamo.

1. INTRODUCTION

The Madison Symmetric Torus (MST) is a large ($R = 1.5$ m, $a = 0.5$ m) toroidal confinement device (Fig. 1) which has been used since August, 1988 to produce reversed-field pinch (RFP) discharges of modest toroidal current ($I < 750$ kA). The toroidal field system will be upgraded during Summer 1993 to allow low-current tokamak operation as well. The MST program is oriented towards evaluating and improving RFP confinement, studying toroidal plasma MHD activity, measuring fluctuation-induced transport, determining the RFP dynamo mechanism, understanding anomalous ion heating, and pursuing concept improvements such as externally applied current drive or profile control.

The RFP differs from the tokamak in the greatly reduced toroidal magnetic field. In the RFP, the toroidal and poloidal components of the magnetic field are comparable ($B_\phi \sim B_\theta$), where in the tokamak, $B_\phi >> B_\theta$. Both components of the RFP magnetic field are powered by the "poloidal field" circuit which drives the toroidal current—the toroidal field is produced by poloidal current in the outer part of the discharge which is driven by a dynamo mechanism. As a result, the direction of the toroidal field reverses on the edge of the plasma. The RFP field geometry has been shown to be a minimum-energy state subject to certain constraints.[1]

The RFP has several advantages over the tokamak

[1]Department of Physics, University of Wisconsin, Madison, Wisconsin 53706.

0164-0313/93/0900-0281$07.00/0

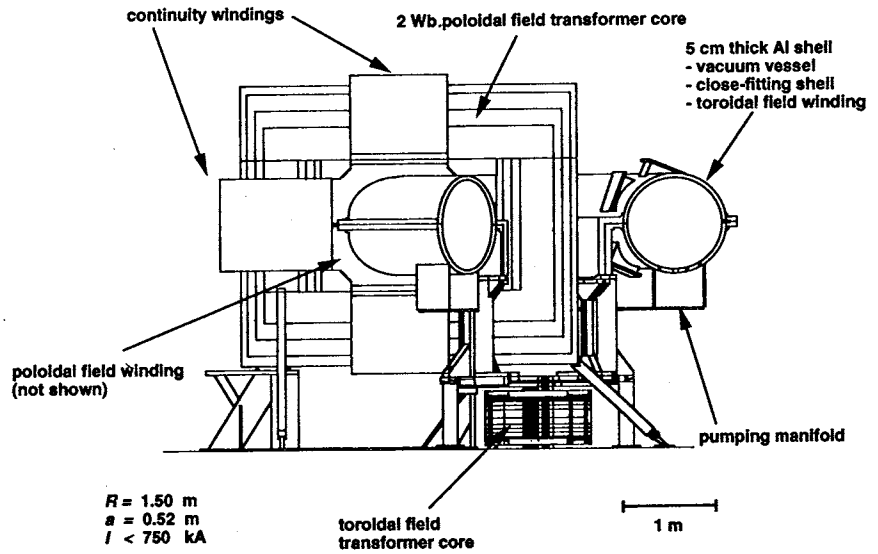

Fig. 1. The Madison Symmetric Torus (MST) can produce large-sized, moderate current RFP plasmas. A unique design feature is the 5 cm thick aluminium shell which also acts as vacuum chamber and toroidal field winding. The toroid is pumped through many small holes to prevent field errors which would be produced around large portholes. The continuity windings allow the shell to carry a continuous toroidal image current without linking the core.

as a fusion reactor concept. The low toroidal field results in very modest toroidal field coil requirements and high plasma beta. The Ohmic power input in the RFP is increased over that of a tokamak due to geometric effects and the dynamo,[2–5] which may also supply the extra power drawn directly by ions in "anomalous" heating.[6–10] As a result, an RFP reactor may reach ignition with only Ohmic power input.[11,12] Its disadvantages include reduced confinement for a given toroidal current due to lower field and larger fluctuation levels, requirement of a close-fitting conducting shell or active feedback to mimic its effect in stabilizing external MHD modes, and the present lack of demonstrated current-drive schemes.

MST has several unique design features.[13] The 5-cm aluminum shell acts as a vacuum vessel, toroidal field winding and close-fitting shell for MHD external mode stability. The plasma is driven by a 2-Wb iron core transformer, which results in the 750 kA limit on toroidal current. MST has very few large port holes, resulting in excellent field uniformity and a high degree of toroidal symmetry. Figure 2 displays waveforms from a typical MST discharge. Due to its large size and core limit, MST has lower toroidal current density ($I/\pi a^2 < 1$ MA/m^2) than most other RFPs.

The role of MST in the worldwide RFP program for its first 5 years of operation (1988–1993) was to investigate RFP confinement at large size, determine the extent of optimization possible by reducing field errors and the vacuum region between the plasma and wall, and to perform detailed measurements of plasma parameters along with magnetic and electrostatic fluctuations for comparison with MHD simulations, turbulent transport theory, anomalous ion heating theories, etc. With the advent of the 2 MA RFX experiment in Padua,[14] which will extend the RFP database to much higher current, the MST effort is changing its concentration in 1993 toward improvement of RFP confinement at low current by means of external profile control, such as electrostatic current injection at the edge or rf techniques, and toward comparison of turbulent transport with similar plasma parameters in tokamak and RFP geometries. This article summarizes MST results from the first 5-year period.

For the purposes of this article, MST results may be divided into the following categories, each treated in a section to follow: RFP confinement, MHD studies, edge fluctuations and transport, anomalous ion heating, and dynamo mechanisms. A brief summary is presented at the end.

2. RFP CONFINEMENT

The RFP is anticipated to perform well as a fusion reactor concept at large current with high plasma beta in

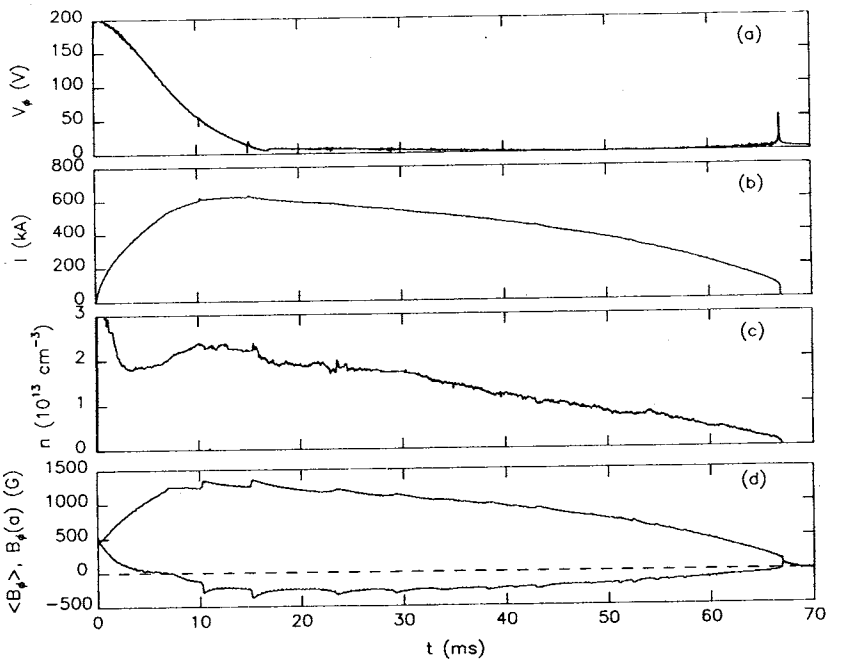

Fig. 2. A typical MST discharge, displaying: (a) applied toroidal voltage, (b) plasma current, (c) line-averaged density, and (d) volume-average and edge toroidal magnetic field. MST is run in "ramped mode," in which the toroidal flux is ramped up from a small initial value by dynamo action. Sudden MHD relaxation events are particularly evident in the toroidal field and represent discrete dynamo activity.

a compact size. The TITAN RFP reactor design[11] has major, minor radii of $R=3.9$ m, $a=0.6$ m, and toroidal current $I=18$ MA with desired poloidal beta $\beta_\theta=20\%$.

The improvement of RFP confinement with increasing toroidal current is based on two principles. First, an RFP is heated Ohmically with power input

$$P_{OH} = \int d^3r \eta j^2 = gI^2 \frac{2R}{a^2}\eta_0 \qquad (1)$$

where

$$g \equiv \left(\frac{\pi a^2 J_0}{I}\right)^2 \int_0^1 \frac{2}{a^2}\, rdr \left(\frac{\eta(r)}{\eta_0}\right)\left(\frac{J(r)}{J_0}\right)^2 \simeq 5 \qquad (2)$$

is a geometric factor which takes into account the electron temperature profile, the current density profile, and the fact that the bulk of Ohmic heating in an RFP is due to poloidal, not toroidal, plasma current; $\eta_0 \propto Z^* T_{e0}^{-3/2}$ is the central Spitzer resistivity with an effective charge Z^* which may include anomalous resistivity enhancement but is assumed to be independent of current and J_0 is the on-axis current density. Second, RFP devices have been able to achieve a beta value of 10% independent of size or current, particularly when they are operated near the empirical high-density radiation limit given by $I/N \sim 2\times10^{-14}$ A-m. (Some devices, such as TPE-1RM20[15] have reported 10% beta values at low density as well.) The beta and density restrictions combine to imply $T \propto I$. As a result, for constant g, Z^* and I/N the Lawson parameter $n\tau_E \propto I^{5/2}$ and the fusion product $n\tau_E T \propto I^{7/2}$, independent of plasma size. With this strong scaling with current, an RFP reaches fusion parameters around the 20 MA level of the TITAN design in a compact size.

MST confinement has been characterized by analyzing a large database (over 600 discharges) which has *independent* variation of current I and density $\bar{n}_e$ (many RFPs are unable to vary density and current independently) with constant magnetic geometry ($F = B_\phi(a)/\langle B_\phi\rangle = -0.16$, $\Theta = B_\theta(a)/\langle B_\phi\rangle = 1.7$). The important parameters, which are fit by power-law relations to I and $\bar{n}_e$ are the central electron temperature, T_{e0}, measured by Thomson scattering; the ion temperature, T_i, measured with a central-chord charge-exchange analyzer[16]; and the resistive part of the toroidal voltage, $V_I = P_{OH}/I$. The trends in these parameters are summarized in Table I. The radiated power fraction is constant around 30% for $I/N > 3\times10^{-14}$ A-m, below which it rises sharply.

Central electron temperature comes closest to following constant beta scaling: at $I/N = 2\times10^{-14}$ A-m, β_e is around 5% in the MST range of currents; however,

Table I. MST Scaling[a]

MST			β = constant
$T_{e0} = 8.3 \times 10^{3}\bar{n}_e^{-0.34}I^{1.09}$	$\propto$	$\left(\frac{I}{N}\right)^{0.34} I^{0.75}$	$\left(\frac{I}{N}\right) I$
$T_i = 4.8 \times 10^{13}\bar{n}_e^{1.25}I^{1.82}$	$\propto$	$\left(\frac{I}{N}\right)^{1.25} I^{0.57}$	$\left(\frac{I}{N}\right) I$
$V_l = 2.7 \times 10^{-5}\bar{n}_e^{0.44}$	$\propto$	$\left(\frac{I}{N}\right)^{-0.44} I^{0.44}$	$Z^* \frac{R}{a^2}\left(\frac{I}{N}\right)^{-3/2} I^{-1/2}$

[a] Temperatures are in eV, density in cm^{-3} and current in kA. The corresponding β = *constant* scaling is also shown for comparison with other RFPs. Exponents have 2–6% uncertainty due to scatter in the data from sawteeth, and other uncontrolled variations.

T_e increases less than linearly with current when *I/N* is held constant, giving a decrease in β_e (we have neglected the contribution of superthermal electrons[17] which are present in in low-density discharges). At fixed current, β_e increases with density, affirming the desirability of operating at the lowest *I/N* value allowed by radiation.

The ion temperature displays a much stronger dependence on current and density and it increases more slowly with current at fixed *I/N* than does the electron temperature. In contrast with electrons, β_i *decreases* with increasing density at fixed current and the decrease of β_i with current at constant *I/N* is stronger. This is because the ions are heated, in part, anomalously ($\tau_{Ei} < \tau_{i/e}$, where $\tau_{i/e}$ is the ion-electron collisional equilibration time) and the data indicates that the anomalous power fraction decreases with increasing density. Fig. 3 displays contours of the anomalous ion heating power fraction

$$\frac{P_{\text{anom}}}{P_i} = 1 - \frac{\nu_{i/e}(T_e - T_i)}{\nu_{Ei}T_i}, \qquad (3)$$

calculated by assuming $\nu_{Ei} = \nu_{Ee} = 0.7/\tau_E$ (the 0.7 accounts for 30% radiated power fraction, assumed constant). The ion temperature will approach the electron temperature at $I > 1$ MA as the electrons and ions become collisionally coupled.

MST plasma resistance does not follow $Z^* = constant$ with increasing current, but measured values of Z^* are in the range 1–4, consistent with the estimated Z_{eff} from impurities, implying that the resistance anomaly is small, in contrast with other RFPs.[15] MST has a close-fitting shell and very low field errors and fluctuation levels, all of which have been blamed for resistance anomalies in other devices.[18–20] The observed increase in Z^* appears to be due to increasing plasma-wall interaction with increasing current.

In summary, MST confinement falls short of the ideal RFP constant beta, constant *I/N* scaling in several ways: the electron beta falls slightly, the ion beta falls more strongly, and Z^* increases with increasing current. RFX will determine whether these trends are inherent in large RFPs or whether confinement improves as current and current density are increased beyond the MST operating range.

There are several factors which degrade the confinement in an RFP. One factor is the quality of the magnetic field at the surface of the plasma—a large radial field error can result in drastic increases in Ohmic power with corresponding reduction of τ_E. In MST, a large radial field error at the vertical gap in the shell accompanies the locking of magnetic oscillations[21] which occurs during a strong MHD relaxation event. This mode locking has been reduced by the use of pre-programmed correction coils in the poloidal field circuit.

Another factor is impurity content. MST has an aluminum plasma-facing shell with small carbon limiters; the dominant impurities are carbon, oxygen and aluminum. Solid-target boronization[22] has effectively been used to reduce the oxygen and aluminum concentration in the discharge. After boronization was begun, long sawtooth-free periods began to appear in low-density discharges with plasma resistance dropping as much as 50% below the typical level between rapid sawteeth. However, these periods generally end in very severe sawteeth accompanied by large impurity bursts.

3. MHD STUDIES

The magnetic field geometry of the RFP leads to the presence of a number of MHD phenomena which have been studied intensively in MST. Tearing modes with poloidal mode number $m = 1$ and toroidal mode numbers $n \sim 2R/a$ are resonant in the plasma interior and are always present.[23,24] These modes usually rotate with poloidal frequency around 20 kHz and are found, using bispectral analysis, to nonlinearly couple to higher, m, n modes as well as to the equilibrium ($m = 0, n = 0$) during sudden MHD relaxation events (sawteeth), similar to $m = 1, n = 1$ sawteeth in tokamaks.[23,24] MST sawteeth are actually discrete dynamo events as they produce a large increase in toroidal flux along with deepened reversal (see Fig. 2). MST has much more severe sawteeth than other RFPs, and they occur under all conditions with varying amplitude and period. It has been suggested that the lower aspect ratio of MST ($R/a = 3$), which leads to a smaller number of resonant internal tearing modes, leads to greater $m = 1$ mode am-

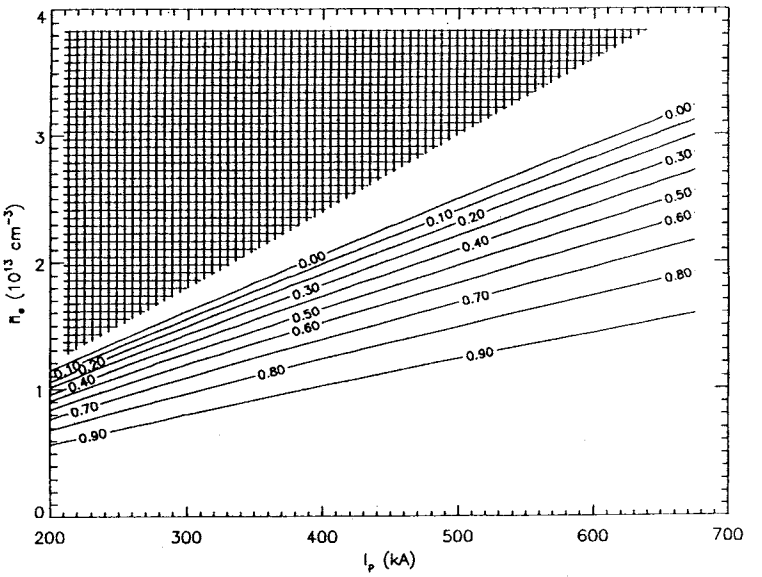

Fig. 3. Contours of constant anomalous ion heating fraction calculated by assuming equal energy loss rates for electrons and ions and constant 30% radiated power fraction. The MST scaling relations displayed in Table I are used to evaluate Eq. (3) as a function of current and density. The hatched region is experimentally inaccessible.

plitude before the nonlinear coupling leads to relaxation. However, HBTX had a similar aspect ratio but smoother, more oscillatory $m = 1$ oscillations without strong $m = 0$ relaxation.[25]

Even though the internally-resonant MHD modes are usually not stationary in the lab frame, the several dominant modes typically maintain phase coherence and form a single, rotating disturbance[21] termed a "slinky" mode when first seen in the OHTE device.[26] In addition to edge magnetic diagnostics, soft X-ray core emission tomography has been used to analyze the radial structure of the mode interaction.[27] The rotating $m = 1$ structure is consistent with linear MHD eigenfunctions; the fast $m = 0$ crash is fairly uniform poloidally and the reconnection topography has not been accurately resolved.

Near the plasma edge, high-frequency, high-n modes are found which are locally resonant such that n changes sign as one crosses the reversal surface with a magnetic probe.[28] Unlike the global, internally resonant modes, these modes display less coherence between modes and shorter spatial coherence lengths.

4. EDGE FLUCTUATIONS AND TRANSPORT

As part of the effort to understand anomalous transport in toroidal confinement devices, the MST group has an unique program in analysis of edge fluctuations and transport. Insertable probes of many types are used in low-current discharges to measure fluctuations in magnetic field, current density, electric potential, plasma density and temperature, and heat flux. Fluctuations in two of these quantities are measured simultaneously in many identical discharges, and the ensemble-averaged correlations are used to extract the contribution to radial particle or energy flux at the edge. For example, the correlated product $\langle \tilde{n}\tilde{\phi} \rangle$ leads to the radial particle flux induced by electrostatic fluctuations.

Electrostatic triple probes have been used to estimate the radial heat and particle flux due to electrostatic fluctuations.[29] The thermal heat flux due to electrostatic fluctuations is found to be small, whereas the particle flux is large enough to qualitatively account for the global particle confinement measured with an H_α diagnostic.

Magnetic probes have been used to estimate the nonambipolar component of radial particle flux due to magnetic fluctuations[28] by measurement of the correlated product $\langle \tilde{j}_\parallel \tilde{B}_r \rangle$. The radial particle transport is found to be ambipolar over the full frequency range encompassing both low-frequency global tearing mode activity and high-frequency locally resonant fluctuations. Given that the radial transport is ambipolar, the total particle flux may be found by measuring $\langle \tilde{j}_{e\parallel} \tilde{B}_r \rangle$, which has been

pursued with the use of an electrostatic electron analyzer probe.[30] The magnetic fluctuation induced flux of fast electrons is a small fraction of the total particle flux.

Radial heat flux due to magnetic fluctuations is proportional to $\langle \tilde{q}_\parallel \tilde{B}_r \rangle$, where $q_\parallel$ is the parallel heat flux, dominated by superthermal electrons in the edge region.[17] A fast pyrobolometer probe has been developed[31] to pursue this measurement, which indicates that the magnetic fluctuation induced heat flux is also a small fraction of the total heat flux. Electrostatic fluctuation induced heat flux due to fast electrons and ions remains to be measured.

5. ANOMALOUS ION HEATING

Ions in present-day RFP plasmas are often heated much more strongly than can be accounted for by classical ion-electron friction.[32,33] We have measured ion heating in MST with a five-channel charge-exchange analyzer (CXA),[16] and CV ion heating with a spectrometer, both with fast time resolution (10 μs), and have found that the ion temperature exhibits rapid increases during discrete dynamo bursts[9,10] (Fig. 4) which are also periods of increased magnetic activity, particularly in low-density discharges where the anomalous ion heating fraction is large. This suggests a heating process which involves transfer of plasma turbulent energy to thermal ion energy. One scenario which has received attention is ion viscous damping[7]; a recently-proposed alternative is that of cyclotron damping of large-k modes.[8] Measurement of the $\tilde{B}$ spectrum in MST indicates an enhancement of fluctuations in the ion cyclotron frequency range during discrete dynamo activity.[9,10] We have not yet been able to rule out any theoretical models; the recent installation of a high-speed Doppler spectrometer capable of measuring toroidal CV velocity fluctuations should provide a test of the viscous damping mechanism.

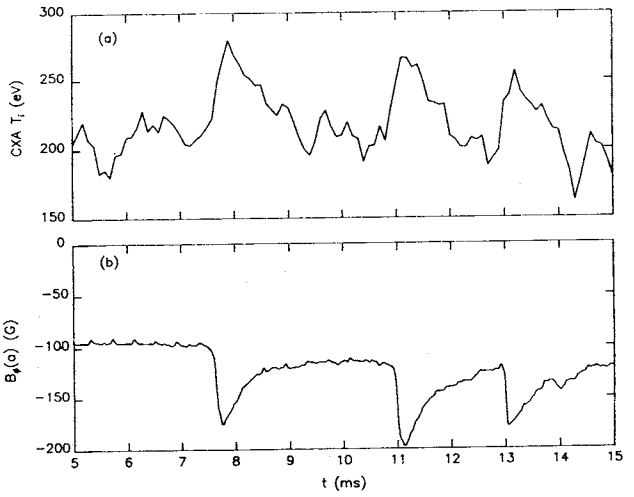

Fig. 4. The ion temperature, measured with a 5-channel charge-exchange analyzer, exhibits sharp increases during strong MHD dynamo activity: (a) ion temperature, (b) edge toroidal magnetic field. Similar behavior is seen in impurity ions.

6. DYNAMO MECHANISMS

The "dynamo" effect in the RFP refers to the plasma's ability to drive poloidal current in the outer region of the plasma, which provides the positive toroidal field in the plasma core and maintains reversal near the edge. The mechanism of the dynamo has not yet been determined experimentally, and MST has an active program with that goal.

If the dynamo is governed by a local relation, it is Ohm's law:

$$\mathbf{E} + \mathbf{V} \times \mathbf{B} = \eta \mathbf{J} + \frac{1}{ne} \mathbf{J} \times \mathbf{B} \qquad (4)$$

where we have included the Hall term. In the outer region of the plasma, $\mathbf{J}$ is predominantly poloidal and cannot be driven by the applied toroidal field, i.e., $\mathbf{E} \cdot \mathbf{J} \sim 0$. The current may be driven by the motion-EMF dynamo term $\mathbf{V} \times \mathbf{B}$ or by other terms such as the Hall term shown above.

In the case of zero equilibrium flow, the motion-EMF term contributes as the spatial or temporal average of a second-order fluctuation product

$$\langle \tilde{\mathbf{V}} \times \tilde{\mathbf{B}} \rangle_\theta = \langle \tilde{V}_r \tilde{B}_\phi \rangle - \langle \tilde{V}_\phi \tilde{B}_r \rangle \qquad (5)$$

We are conducting measurements of this term in the plasma edge using probe techniques developed on the REPUTE RFP[34] and the SPHEX spheromak.[35] The $\langle \tilde{V}_\phi \tilde{B}_r \rangle$ term is being measured further into the plasma by the high-speed CV Doppler spectrometer for $\tilde{V}_\phi$.

A magnetic probe diagnostic has been used to measure the fluctuation Hall term $\langle \tilde{\mathbf{J}} \times \tilde{\mathbf{B}} \rangle$ in the plasma edge.[36] It is found to be non-negligible, but can account for no more than 25% of the dynamo-driven current.

An alternative, nonlocal description of the dynamo attributes the poloidal current in the edge to superthermal electrons which are generated in the core and rapidly transport outward.[37] A large fraction of the edge current is indeed found to be carried by superthermal elec-

trons.[17,30] In addition, a small fraction of superthermal electrons is observed in the core,[17] particularly in low-density discharges with high values of E/E_c, where E_c is the critical field for electron runaway. We have an ongoing program of experiments to measure the contribution of superthermal electrons to the dynamo and determine their generation and transport mechanism.

7. SUMMARY

An extensive program of research is carried out on MST to study the underlying physics of RFP confinement, MHD activity, fluctuations and transport, ion heating and dynamo mechanisms. MST has proven to be a good device for these studies, as it allows independent variation of parameters such as current and density. MST confinement has fallen short of the scaling trends observed in smaller RFPs; the RFX experiment in Italy will be able to perform measurements at current densities comparable to small RFPs at the size of MST. Meanwhile, the MST program will shift orientation from conventional RFP studies to comparison of fluctuations and transport in both tokamak and RFP geometry, made possible by a toroidal field upgrade in the second half of 1993, and improvement of the RFP by active profile control using insertable electrodes and rf current drive. In this way, we hope to improve understanding of plasma heating, confinement, and transport in toroidally-confined plasmas, regardless of geometry, and further advance the RFP concept.

ACKNOWLEDGMENTS

This work was supported by the U.S. Department of Energy.

REFERENCES

1. J. B. Taylor (1986). *Rev. Mod. Phys.* **58,** 741.
2. J. W. Johnson (1981). *Plasma Phys.* **23,** 187.
3. K. F. Schoenberg, R. F. Gribble, and J. A. Phillips (1982). *Nucl. Fusion* **22,** 1433.
4. J. C. Sprott (1988). *Phys. Fluids* **31,** 2266.
5. W. Shen and J. C. Sprott (1991). *Phys. Fluids B* **3,** 1225.
6. C. G. Gimblett (1990). *Europhys. Lett.* **11,** 541.
7. Z. Yoshida (1991). *Nucl. Fusion* **31,** 386.
8. N. Mattor, S. C. Prager, and P. Terry (1993). *Comments Plasma Phys. Contr. Fusion* **15,** 65.
9. E. Scime, S. Hokin, N. Mattor, and C. Watts (1992). *Phys. Rev. Lett.* **68,** 2165.
10. E. Scime, M. Cekic, D. J. Den Hartog, S. Hokin, D. Holly, and C. Watts (1992). *Phys. Fluids B* **4,** 4062.
11. F. Najmabadi *et al.* (1990). UCLA Report UCLA-PPG-1200, UCLA.
12. K. A. Werley (1991). *Nucl. Fusion* **31,** 567.
13. R. N. Dexter, D. Kerst, T. W. Lovell, S. C. Prager, and J. C. Sprott (1991). *Fus. Technol.* **19,** 131.
14. G. Malesani (1987). in *Proceedings of the International School of Plasma Physics Workshop on Physics of Mirrors, Reversed Field Pinches and Compact Tori, Varenna, Italy, 1986.* S. Ortolani and E. Sindoni (eds.) (Società Italiana di Fisica, Bologna) p. 359.
15. Y. Yagi, Y. Maejima, Y. Hirano, T. Shimada, K. Hattori, I. Hirota, and P. R Brunsell (1992). *Plasma Physics and Controlled Nuclear Fusion Research, 1992.* International Atomic Energy Agency, Vienna. To be published.
16. Earl Scime and Samuel Hokin (1992). *Rev. Sci. Instrum.* **63,** 4527.
17. S. Hokin, A. Almagri, S. Assadi, M. Cekic, B. Chapman, G. Chartas, N. Crocker, M. Cudzinovic, D. J. Den Hartog, R. Dexter, G. Fiksel, J. Henry, D. Holly, S. Prager, T. Rempel, J. Sarff, E. Scime, W. Shen, C. Sprott, M. Stoneking, and C. Watts (1992). *Plasma Physics and Controlled Nuclear Fusion Research, 1992.* International Atomic Energy Agency, Vienna. To be published.
18. K. F. Schoenberg, R. W. Moses, and R. L. Hagenson (1984). *Phys. Fluids* **27,** 1671.
19. T. R. Jarboe and B. Alper (1987). *Phys. Fluids* **30,** 1177.
20. H. Y. W. Tsui (1988). *Nucl. Fusion* **28,** 1543.
21. A. F. Almagri, S. Assadi, S. C. Prager, J. S. Sarff, and D. W. Kerst (1992). *Phys. Fluids B* **4,** 4080.
22. D. J. Den Hartog, M. Cekic, G. Fiksel, S. Hokin, R. Kendrick, S. Prager, and M. Stoneking (1993). *J. Nucl. Mater.* **200,** 177.
23. S. Assadi, S. C. Prager, and K. L. Sidikman (1992). *Phys. Rev. Lett.* **69,** 281.
24. J. Sarff, S. Assadi, A. Almagri, M. Cekic, D. J. Den Hartog, G. Fiksel, S. Hokin, H. Ji, S. Prager, W. Shen, K. Sidikman, and M. Stoneking (1993). *Phys. Fluids B* **5,** 2540.
25. R. J. Hayden and B. Alper (1989). *Plasma Phys. Controlled Fusion* **31,** 193.
26. T. Tamano, W. D. Bard, C. Chu, Y. Kondoh, R. J. LaHaye, P. S. Lee, M. T. Saito, M. J. Schaffer, and P. L. Taylor (1987). *Phys. Rev. Lett.* **59,** 1444.
27. George Chartas and Samuel Hokin (1992). *Phys. Fluids B* **4,** 4019.
28. W. Shen, R. N. Dexter, and S. C. Prager (1992). *Phys. Rev. Lett* **68,** 1319.
29. T. D. Rempel, C. W. Spragins, S. C. Prager, S. Assadi, D. J. Den Hartog, and S. A. Hokin (1991). *Phys. Rev. Lett.* **67,** 1438.
30. T. D. Rempel, A. F. Almagri, S. Assadi, D. J. Den Hartog, S. A. Hokin, S. C. Prager, J. S. Sarff, W. Shen, K. L. Sidikman, C. W. Spragins, J. C. Sprott, M. R. Stoneking, and E. J. Zita (1992). *Phys. Fluids B* **4,** 2136.
31. G. Fiksel, J. Frank, and D. Holly (1993). *Rev. Sci. Instrum.* Submitted.
32. P. G. Carolan, A. R. Field, A. Lazaros, M. G. Rusbridge, H. Y. W. Tsui, and M. V. Bevir (1987). *Proceedings of the 14th European Conf. on Contr. Fusion and Plasma Physics, Madrid,* EPS, Petit-Lancy, Vol. 2, p. 469.
33. G. A. Wurden *et al.* (1988). *Proceedings of the 15th European Conf. on Contr. Fusion and Plasma Physics, Dubrovnik,* EPS, Petit-Lancy, p. 331.
34. H. Ji, H. Toyama, A. Fujisawa, S. Shinohara, and K. Miyamoto (1992). *Phys. Rev. Lett.* **69,** 616.
35. A. al-Karkhy, P. K. Browning, G. Cunningham, S. J. Gee, and M. G. Rusbridge (1993). *Phys. Rev. Lett.* **70,** 1814.
36. W. Shen and S. C. Prager (1993). *Phys. Fluids B* **5,** 1931.
37. A. R. Jacobson and R. W. Moses, Jr. (1984). *Phys. Rev. A* **29,** 3335.